Supplemental figure legends:

Figure S1: Bt-549 cells produce Src-dependent invadopodia. Bt-549 breast cancer cells were plated on fluorescent gelatin, and invadopodia were observable by 4 hours. Focal degradation was blocked completely by c-Src inhibition with SU6656.

Figure S2: Bt-549 cells produce microtentacles that are enhanced by c-Src inhibition. Acute exposure of Bt-549 cells significantly increased McTN formation, in a manner consistent with that seen in MDA-231s. (* indicates significant change relative to MDA-231 parental cells; $p < 0.001$)

Figure S3: SU6656-mediated suppression of invadopodia is represented quantitatively as a loss of focal degradation, and is most pronounced in the c-Src-527 cells. Values are expressed as percentage of total cell area degraded (* denotes significant changes relative to vehicle control, $p<0.5$).

Figure S4: Differential regulation of C-Src upon detachment: MDA-231 cells and c-Src variants were cultured on a gelatin-coated tissue culture surface and incubated at 37º. Half of these cells were trypsinized at 195 minutes, suspended over a low attachment surface for 45 minutes and then pelleted by centrifugation. At 4h, both the adherent (A) cells and the suspension (S) cell pellets were lysed in equal volume of lysis buffer, and subjected to SDS-PAGE. Antibodies against activated src (pY Src), and total src showed that Src activity is affected by detachment. Beta actin served as a loading control.

Figure S5: *In vitro* attachment is enhanced by changes in c-Src activity and microtentacle formation. Approximately 5,000 cells were plated, in quadruplicate, in each well of a Roche Xcelligence e-plate, and cell attachment was analyzed in real-time by electrical impedance recordings every 15 seconds for a total time of 1 hour. During the first 20 minutes, both c-

Src527 and c-Src295 adhered more rapidly than parental MDA-231 cells, indicating a period of initial attachment that is independent of cell spreading and establishment of permanent substrate contacts. A representative trend is shown (duplicated over multiple independent trials; n=4).

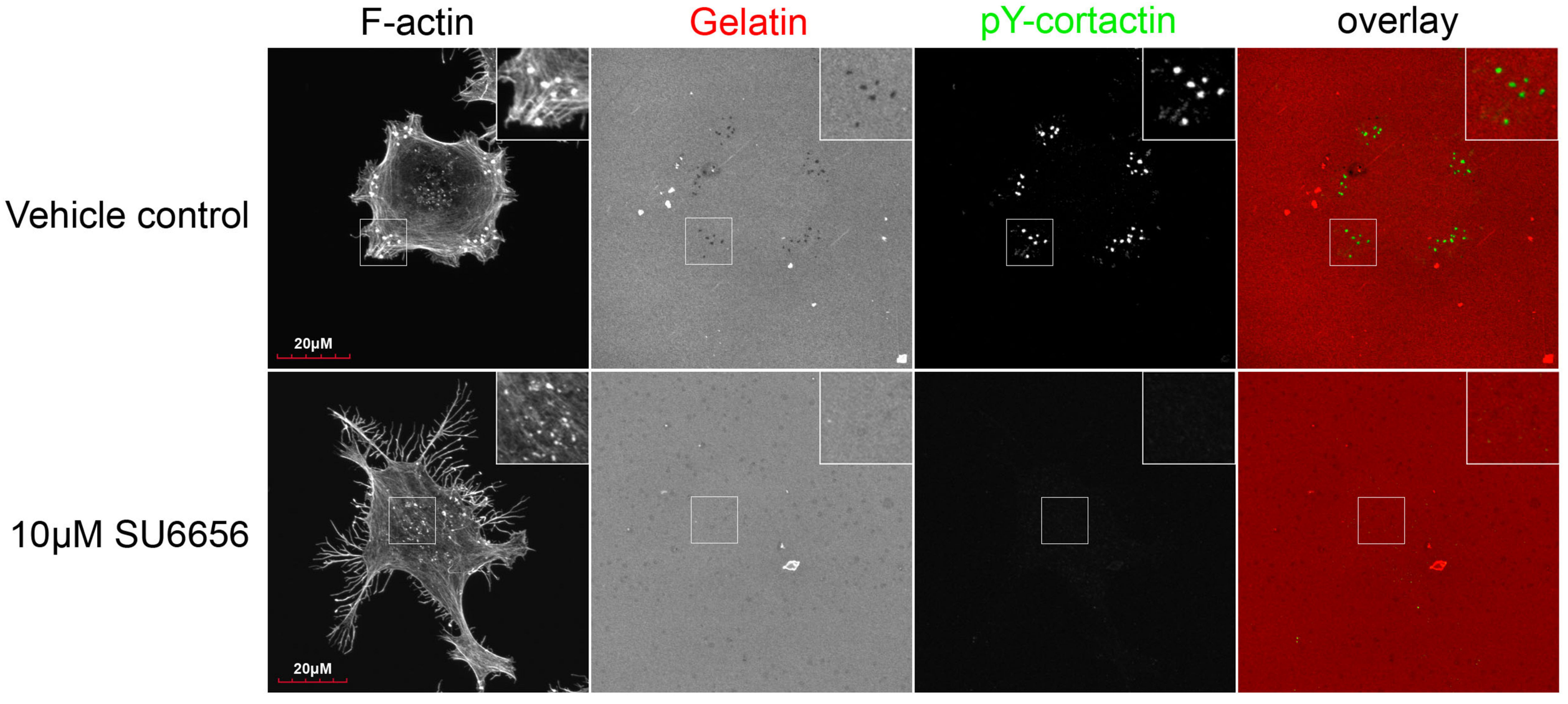
F-actin
Gelatin
pY-cortactin
overlay
Vehicle control
10μM SU6656
20μM
20μM

α-tubulin

F-actin

overlay

10μM SU6656

MDA-MB-231

10μM

-

+

c-Src 527

-

+

c-Src 295

-

+

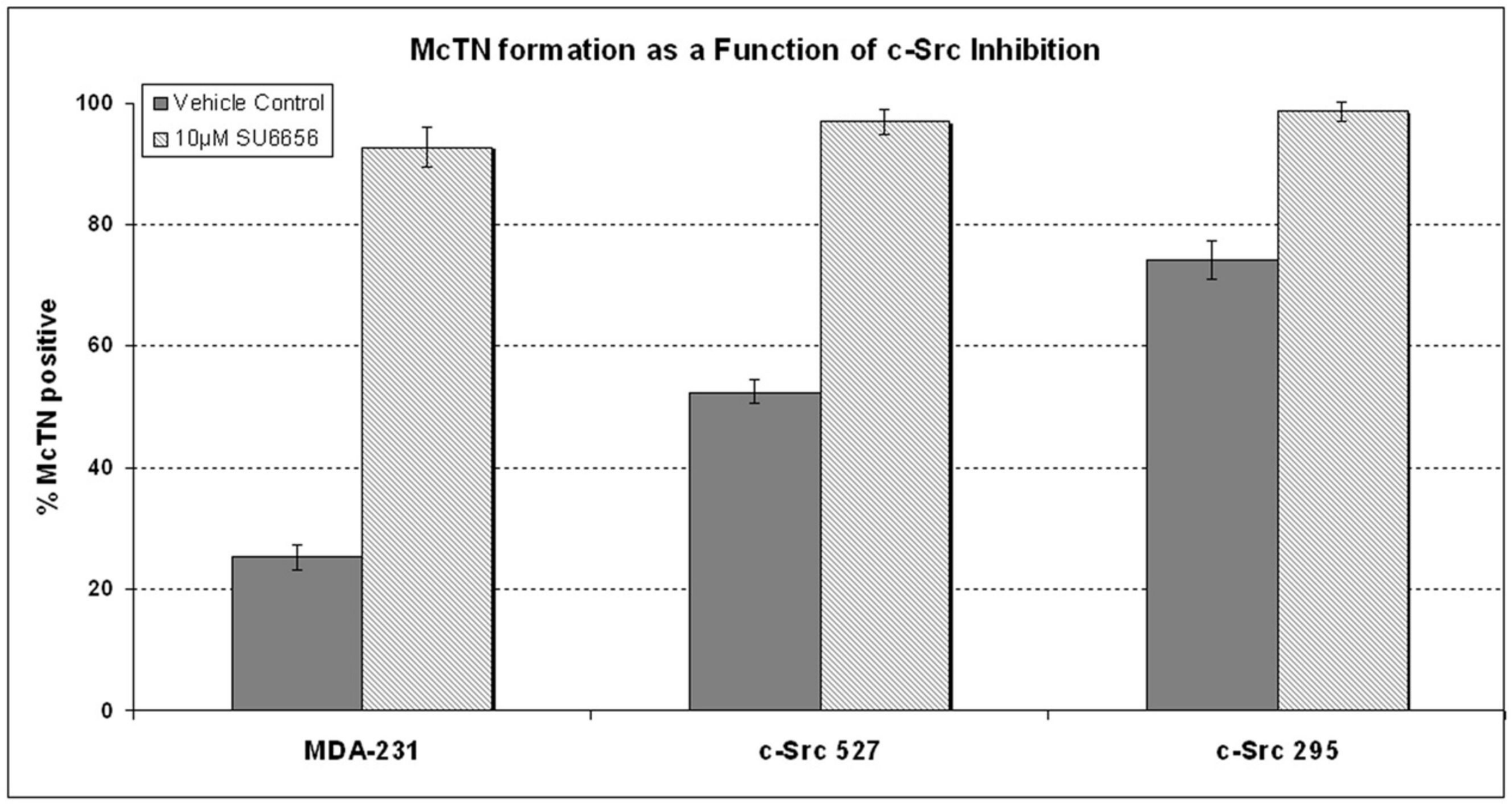
McTN formation as a Function of c-Src Inhibition
Vehicle Control
10μM SU6656
% McTN positive
100
80
60
40
20
0
MDA-231
c-Src 527
c-Src 295

ns control

Tks5 shRNA

NIH 3T3

Src3T3

Src 3T3 C1

Src 3T3 C2

Src 3T3 4.20

Src 3T3 4.24

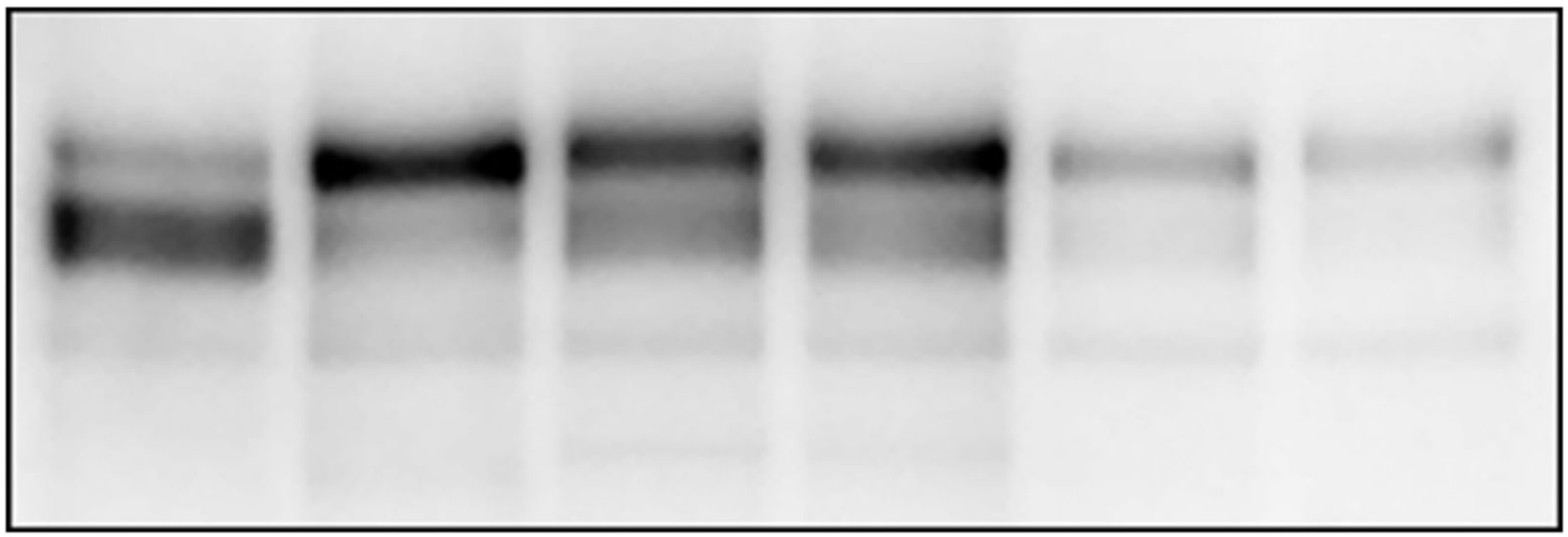

-150kD

Tks5/Fish

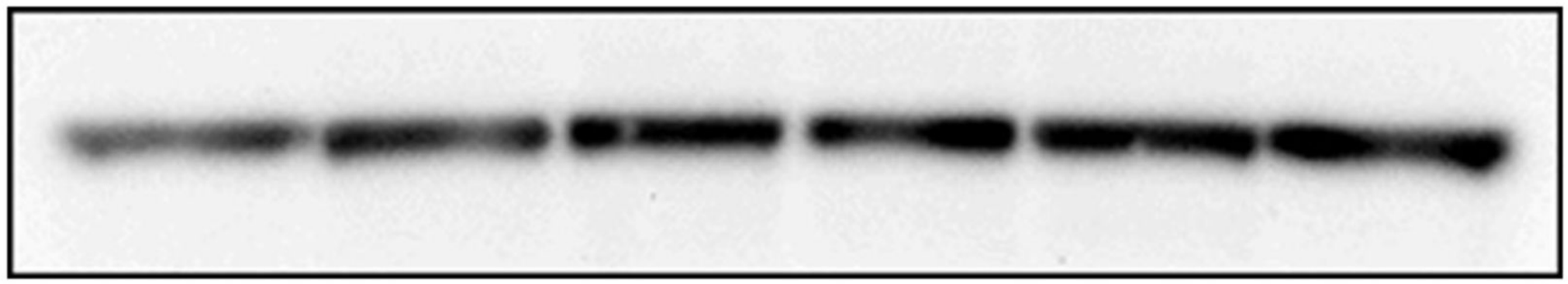

Beta-actin

F-actin

gelatin

Tks5/Fish

overlay

Src 3T3

Src 3T3 C1

Src 3T3 4.24

10μM

10μM

10μM

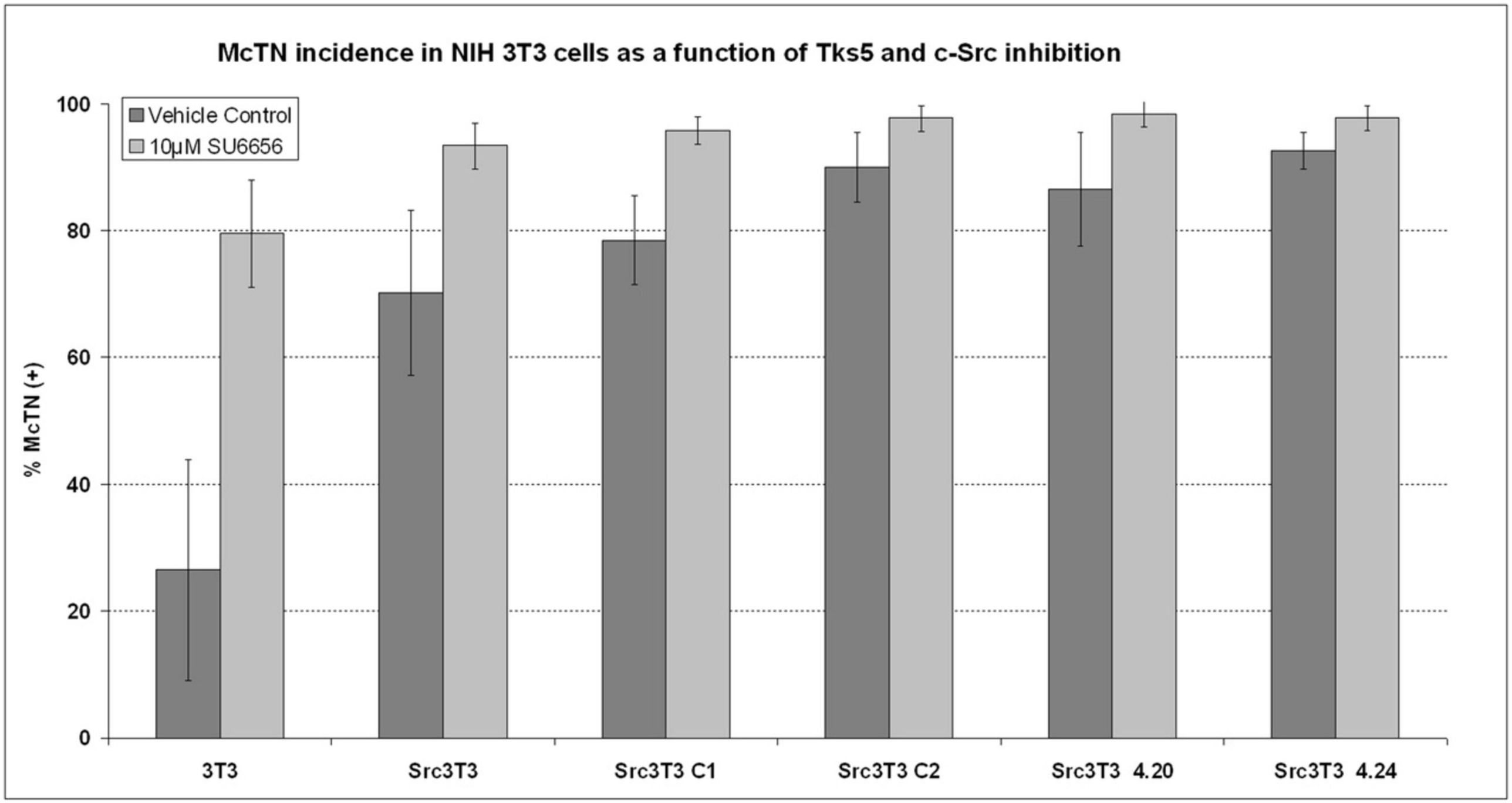
McTN incidence in NIH 3T3 cells as a function of Tks5 and c-Src inhibition
Vehicle Control
10μM SU6656
% McTN (+)
100
80
60
40
20
0
3T3
Src3T3
Src3T3 C1
Src3T3 C2
Src3T3 4.20
Src3T3 4.24

Lung Retention of Circulating Tumor Cells as a function of c-Src activity

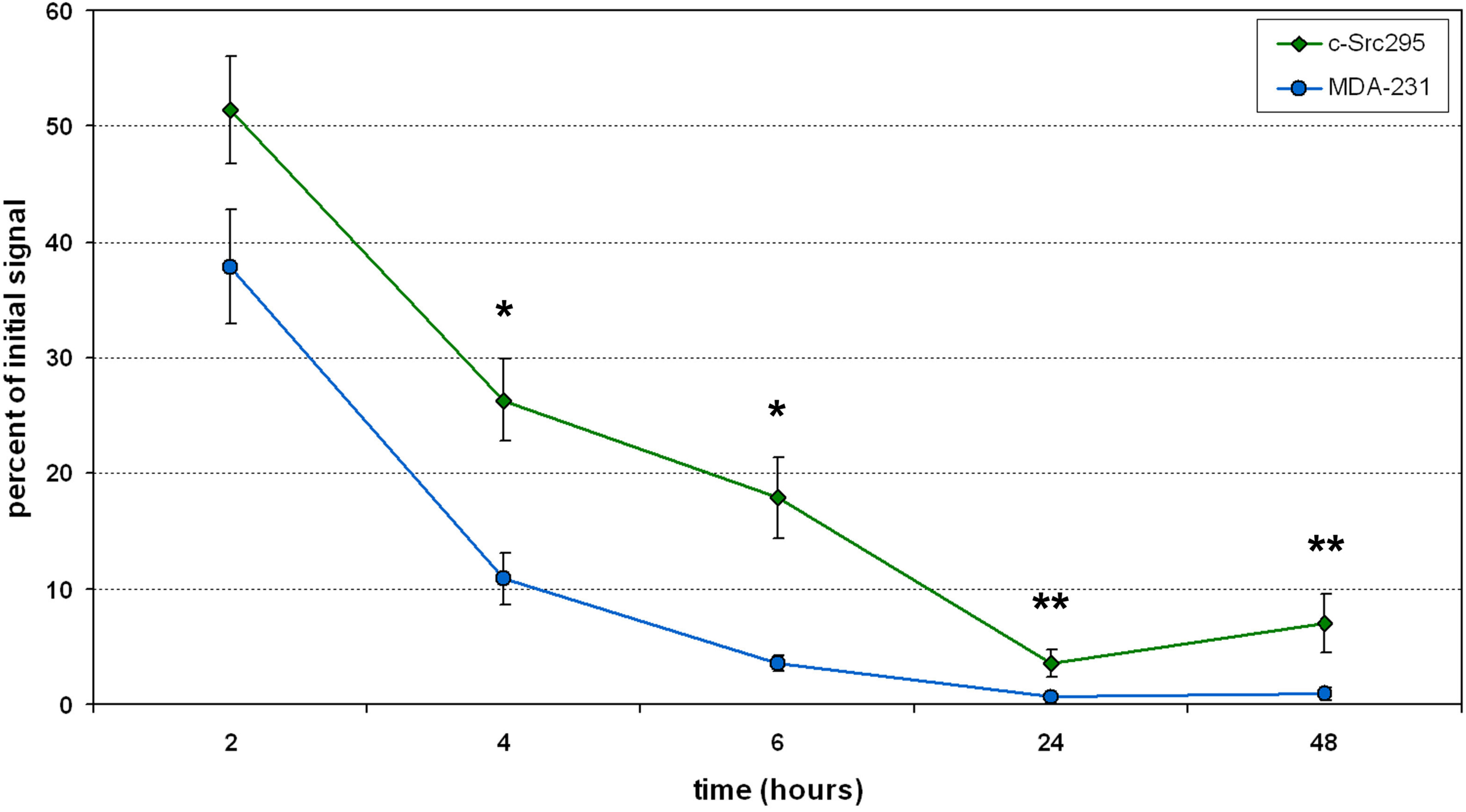

Initial

2h

4h

6h

MDA-231

c-Src 295